PERGAMON

Atmospheric Environment 36 (2002) 527–536

ATMOSPHERIC ENVIRONMENT

www.elsevier.com/locate/atmosenv

On the escape of pollutants from urban street canyons

Jong-Jin Baik*, Jae-Jin Kim

Department of Environmental Science and Engineering, Kwangju Institute of Science and Technology, Kwangju 500-712, South Korea

Received 3 May 2001; received in revised form 13 August 2001; accepted 24 August 2001

Abstract

Pollutant transport from urban street canyons is numerically investigated using a two-dimensional flow and dispersion model. The ambient wind blows perpendicular to the street and passive pollutants are released at the street level. Results from the control experiment with a street aspect ratio of 1 show that at the roof level of the street canyon, the vertical turbulent flux of pollutants is upward everywhere and the vertical flux of pollutants by mean flow is upward or downward. The horizontally integrated vertical flux of pollutants by mean flow at the roof level of the street canyon is downward and its magnitude is much smaller than that by turbulent process. These results indicate that pollutants escape from the street canyon mainly by turbulent process and that the net effect of mean flow is to make some escaped pollutants reenter the street canyon. Further experiments with different inflow turbulence intensities, inflow wind speeds, and street aspect ratio confirm the findings from the control experiment. In the case of two isolated buildings, the horizontally integrated vertical flux of pollutants by mean flow is upward due to flow separation but the other main results are the same as those from the control experiment.

Keywords: Flow and dispersion; Urban street canyon; Pollutant transport; Vertical turbulent flux of pollutants

1. Introduction

Flow and dispersion in urban canopies are very complicated because of complex building configurations and ever-changing meteorological conditions. Extensive studies on the flow and dispersion in urban canopies have been conducted to improve our understanding, accurately predict them and minimize the damage associated with harmful pollutants, and help urban planners to take into account urban geometry with optimal natural ventilation and comfort. These include studies on flow regimes (e.g., Hunter et al., 1992; Baik and Kim, 1999) and dispersion (e.g., Wedding et al., 1977; Hoydysh and Dabberdt, 1988; Meroney et al., 1996; Kastner-Klein et al., 2000) in urban street canyons, thermal effects on urban street-canyon flow and dispersion (e.g., Sini et al., 1996; Kim and Baik, 1999; Uehara et al., 2000), and so on. Among the many subjects investigated previously, the topic of pollutant transport from urban street canyons is particularly important because of its connection with natural ventilation and its applicability to urban air quality models as well as its fluid-dynamical implications.

In an analytical model to estimate pollutant concentration in the street canyon, Hotchkiss and Harlow (1973) assumed that the pollutant transport to the ambient air is determined by the turbulent eddy diffusivity within the canyon. On the other hand, Nicholson (1975) developed an analytical pollution model under the assumption that the mean concentration of street-level air is governed by the mean updraft velocity at the roof level on the upwind side of the street canyon. In a field study, DePaul and Sheih (1985) tried to estimate the exchange rate of pollutants between the street canyon and the upper air. They found that the ventilation velocity, which represents an average velocity of pollutants transported from the canyon and is calculated using pollutant retention time and wind speed, ranges from 15 to 80 cm s^{-1}. The ventilation

*Corresponding author. Present address: School of Earth and Environmental Sciences, Seoul National University, Seoul 151-742, South Korea.

E-mail address: chy@atmos.yonsei.ac.kr (J.-J. Baik).

1352-2310/02/$ - see front matter
PII: S1352-2310(01)00438-1

velocity was found to be well correlated with the friction velocity at the roof level, which in turn is related to the vertical turbulent flux of pollutants at the roof level. Using a numerical model, Lee and Park (1994) examined the exchange rate of pollutants between the street canyon and the upper air. They parameterized a time constant, defined as the time required for the average pollutant concentration in the street canyon to be reduced to e^{-1}, as a function of canyon cross-sectional area, influx strength, Reynolds number, Peclet number, and street aspect ratio.

Despite our understanding of the factors and processes responsible for pollutant transport from street canyons owing to the efforts of previous studies, there appears to be some controversy regarding the process responsible. Moreover, to our knowledge, no attempts have been made to estimate to what extent the vertical turbulent flux of pollutants dominates the vertical flux of pollutants by mean flow at the roof level of the street canyon or vice versa. This study aims at investigating these problems through numerical model simulations.

The numerical model used in this study is described in Section 2. In Section 3, the numerical model is validated against the data from water-channel and wind-tunnel experiments. Results of pollutant escape from urban street canyons are presented and discussed in Section 4. Finally, summary and conclusion are given in Section 5.

2. Numerical model

The airflow system considered in this study is a two-dimensional (x–z plane), nonhydrostatic, nonrotating, incompressible system. The governing equation set is Reynolds-averaged in Cartesian coordinates and includes the horizontal momentum equation, the vertical momentum equation, the mass continuity equation, and the transport equation for pollutant concentration. Turbulent processes for momentum and pollutants are treated with the equations for turbulent kinetic energy and dissipation rate ($k-\varepsilon$ turbulence closure scheme). The governing equations are numerically solved on a staggered grid system using the finite volume method (Patankar, 1980). For further details of the numerical model, see Baik and Kim (1999).

The horizontal and vertical domain sizes are 100 and 120 m, respectively, and the grid resolution is 1 m in both directions. The time step is 0.05 s. The building height is 40 m and the width between two buildings is also 40 m. Hence, the street aspect ratio, defined by the ratio of the building height to the width between two buildings, is one. The ambient wind blows from left to right, thus the left and right buildings are referred to as the upwind and downwind buildings, respectively (see Fig. 3). The inflow wind profile is given by

$$U_{\mathrm{i}} = U_{\mathrm{r}}\left(\frac{z}{z_{\mathrm{r}}}\right)^{0.299}, \tag{1}$$

where z_{r} and U_{r} are specified as 10 m and 2.5 m s^{-1}, respectively. This power-law profile yields inflow wind speeds of 3.78 m s^{-1} at the building roof level ($z = 40$ m) and 5.26 m s^{-1} at the model top ($z = 120$ m). The inflow turbulent kinetic energy profile is represented by

$$k_{\mathrm{i}} = aU_{\mathrm{i}}^2, \tag{2}$$

where a is a parameter that controls the inflow turbulence intensity and specified as 0.005. Therefore, the ratio of the inflow turbulent kinetic energy to the inflow mean kinetic energy is 0.01. The inflow dissipation rate profile is given by

$$\varepsilon_{\mathrm{i}} = \frac{C_\mu^{3/4} k_{\mathrm{i}}^{3/2}}{\kappa z}, \tag{3}$$

where C_μ is a constant ($=0.09$) and κ is the von Karman constant ($=0.4$). The inflow wind speed (U_{i}), turbulent kinetic energy (k_{i}), and dissipation rate (ε_{i}) profiles at the model left (inflow) boundary remain the same during the model integration. The numerical model is integrated up to $t = 2$ h. At $t = 1$ h, the mean flow and turbulent kinetic energy at each grid point had already reached a quasi-steady state. The mean and turbulent flow fields presented below are at $t = 1$ h. Starting from $t = 1$ h, passive pollutants are continuously released at street-level grid points (40 points) at a rate of 5 ppb s^{-1}.

The parameters given above are for the control experiment, results of which are shown in Figs. 3–9. The parameters used for other experiments are the same as those for the control experiment, except for the parameter value that will be specifically mentioned in Section 4.

3. Model validation

In this section, flow and pollutant concentration fields in an urban street canyon simulated using the numerical model (control experiment) are validated against some fluid-experimental data. For the comparison of flow fields, a physical experiment is conducted using a circulating water channel constructed to investigate urban street-canyon flows (Baik et al., 2000). Two model buildings, separated by 10 cm, are mounted on the water channel. Each model building is 10 cm high (hence, the street aspect ratio is 1) and 40 cm wide. This rather wide building width is considered to make inflow near the entrance region of the canyon parallel to the bottom. The depth of water is 30 cm. For details of the apparatus, see Odell and Kovasznay (1971) and Baik et al. (2000). Fig. 1 shows the vertical profiles of the normalized vertical velocity at upwind ($x_{\mathrm{d}}/D = 0.15$,

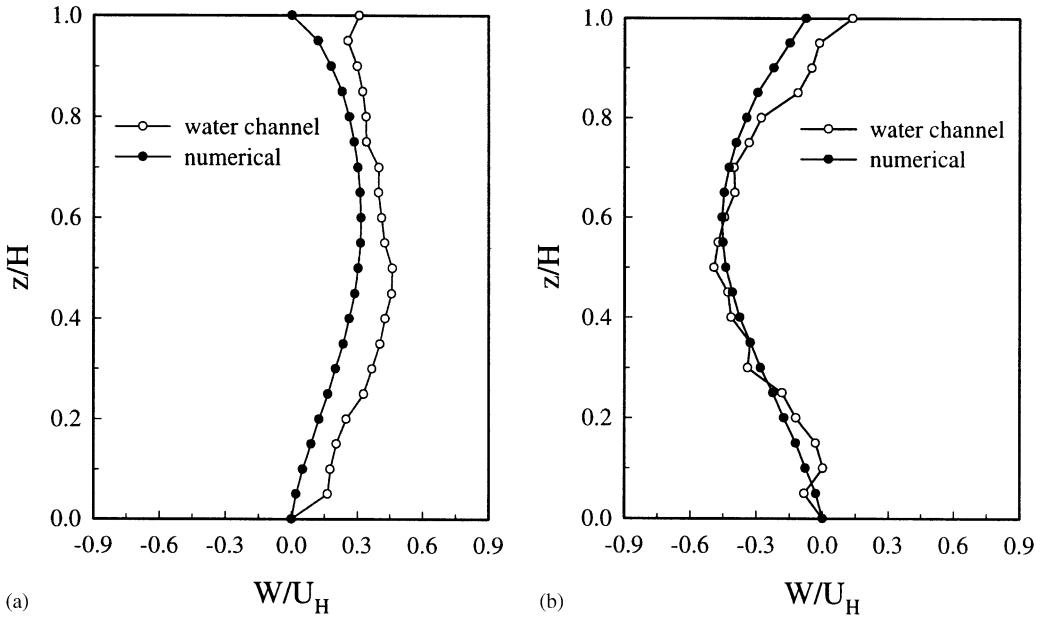

Fig. 1. Vertical profiles of normalized vertical velocity at (a) upwind ($x_d/D = 0.15$, where x_d is the horizontal distance from the upwind building corner and D is the width between the buildings) and (b) downwind ($x_d/D = 0.85$) locations of the model street canyon in the circulating water-channel and numerical experiments. The vertical velocity is normalized by the local horizontal velocity at the top of the middle street canyon (U_H) and the height is normalized by the model building height (H).

where x_d is the horizontal distance from the upwind building corner and D is the width between the buildings) and downwind ($x_d/D = 0.85$) locations of the model street canyon in the circulating water channel and numerical experiments. The vertical velocity is normalized by the horizontal velocity at the top of the mid-canyon (U_H) and the height is normalized by the model building height (H). In each experiment, in association with the circulation of a single vortex formed in the street canyon, upward motion is observed on the upwind side of the street canyon and downward motion on the downwind side. At each location, the vertical profile of the normalized vertical velocity in the numerical experiment is similar to that in the water-channel experiment. The two vertical profiles of the normalized vertical velocity are closer to each other at the downwind location than at the upwind location.

To compare pollutant concentrations, the data obtained by wind-tunnel experiment (Meroney et al., 1996) are used. The data taken from their study are for the urban roughness case in which the vortex is trapped within the canyon. In the numerical experiment, pollutants are released at the middle point of the street to be consistent with their line source. The pollutant emission rate is $200\,\mathrm{ppb\,s^{-1}}$. Fourteen measurement locations are shown in Fig. 4a of their paper. Fig. 2 shows normalized pollutant concentrations at 11 locations in the wind-tunnel experiment and corresponding

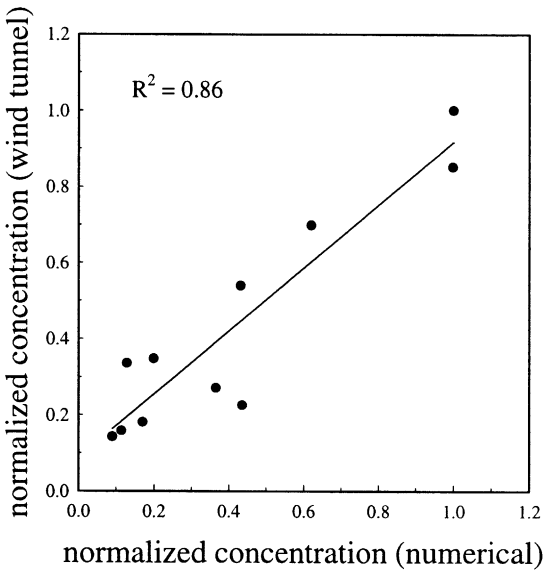

Fig. 2. Normalized pollutant concentrations at 11 locations in the wind-tunnel experiment of Meroney et al. (1996) and corresponding normalized pollutant concentrations in the numerical experiment. The 11 locations are $z/H = 0.17$, 0.33, 0.67, and 0.97 on the faces of the upwind and downwind buildings and $x_d/D = 1.25$, 1.50, and 1.75 on the top face of the downwind building. The pollutant concentration is normalized by its value at location 7.

ones in the numerical experiment. The pollutant concentration is normalized by the concentration at location 7 (face of the upwind building at $z/H = 0.17$) that shows the highest value among the chosen 11 locations. The three locations (measurement locations 1–3) in Meroney et al. (1996) are not included in this figure because the flow above the upwind model building is parallel to the ground and accordingly pollutants penetrate insignificantly into the region just above the upwind building due to the absence of a reversed flow there. The normalized pollutant concentration in the numerical experiment is linearly well correlated with that in the wind-tunnel experiment, with R^2 being 0.86. A good agreement between the numerical and fluid experiments as shown in Figs. 1 and 2 will reliably support the physical realism of numerical model results presented in the next section.

4. Results and discussion

First, the fields of mean flow and turbulent kinetic energy within the street canyon are briefly presented. The streamline field (Fig. 3) shows a well-organized, clockwise-rotating vortex within the canyon. The vortex center is located at a downwind and upward position ($x = 54$ m, $z = 25$ m) from the canyon center ($x = 50$ m, $z = 20$ m). This downwind shift of the vortex center is, by mass conservation, associated with the stronger vertical velocity near the downwind building than near the upwind building (see Fig. 4b). These results are consistent with those of previous studies (e.g., Lee and Park, 1994). The vertical profiles of the horizontal and vertical velocities at $x = 34$ m (an upwind location), 54 m (vortex-center location), and 66 m (a downwind location) shown in Figs. 4a and b reflect the circulation of the vortex trapped within the canyon. The horizontal velocity at the downwind location is stronger than that at the upwind location and the downward motion at the downwind location is stronger than the upward motion at the upwind location. The turbulent kinetic energy (Fig. 4c) is large near the roof level owing to the strong velocity shear there. At the downwind location, the turbulent kinetic energy increases with height.

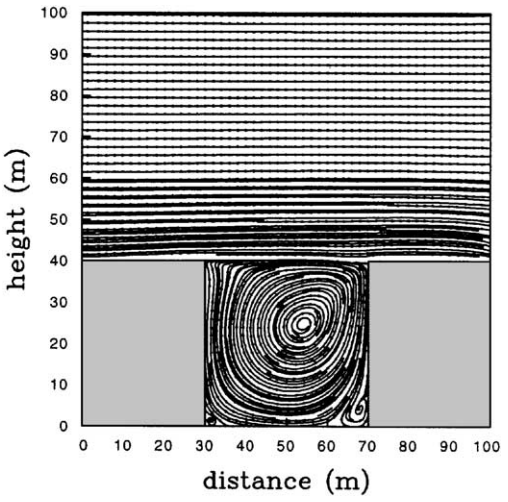

Fig. 3. Streamline field at $t = 1$ h. Note that Figs. 3–9 are for the control experiment.

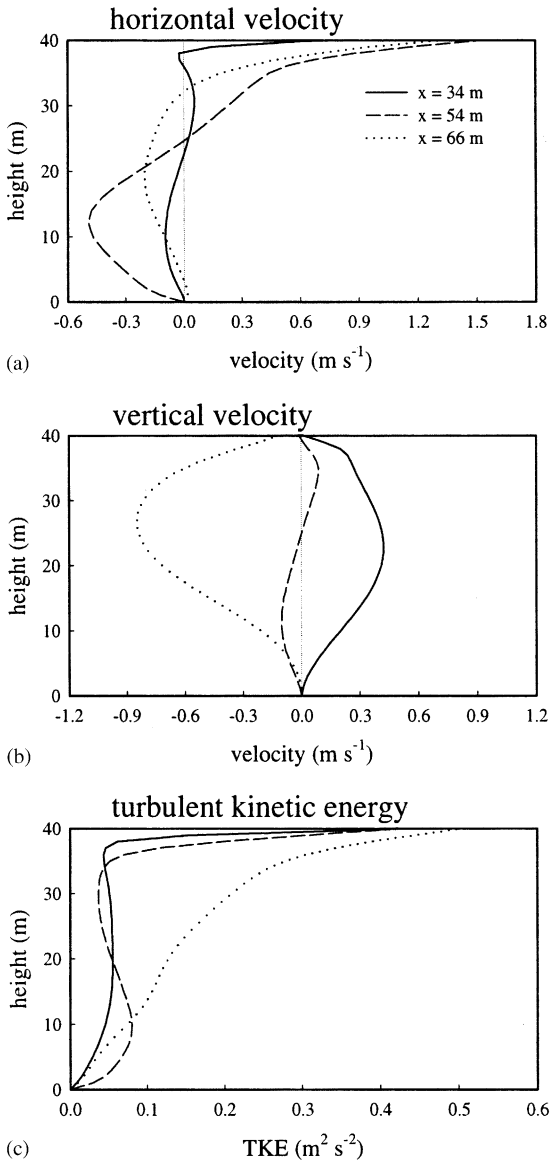

Fig. 4. Vertical profiles of (a) horizontal velocity, (b) vertical velocity, and (c) turbulent kinetic energy at $x = 34$ m (solid line), 54 m (dashed line), and 66 m (dotted line). These are at $t = 1$ h.

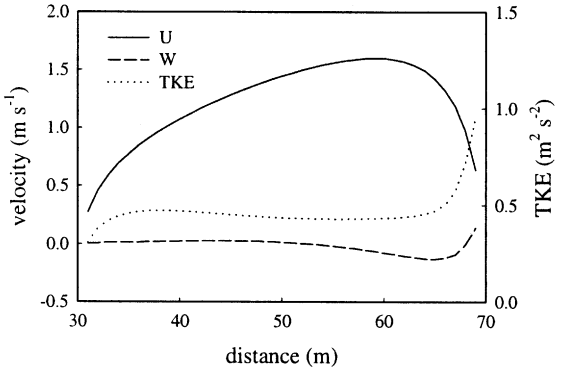

Fig. 5. Horizontal distributions of horizontal velocity (solid line), vertical velocity (dashed line), and turbulent kinetic energy (dotted line) at $z = 40$ m. These are at $t = 1$ h.

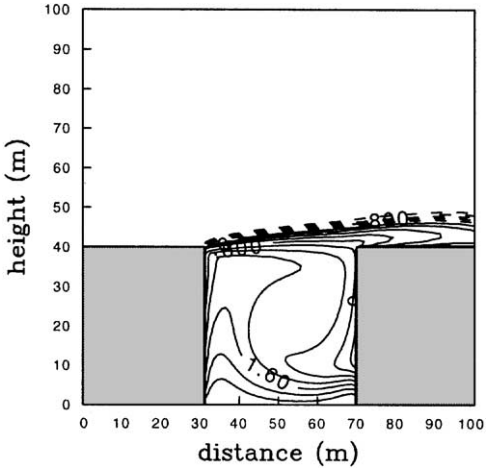

Fig. 6. Pollutant concentration field (log scale in base 10) at $t = 2$ h. The unit is ppb and the contour interval is 0.2.

At the top of the street canyon ($z = 40$ m), the horizontal wind speed gradually increases from the upwind building edge to a downwind position of $x = 60$ m and then rather rapidly decreases up to the downwind building edge (Fig. 5). The updraft on the upwind side of the vortex center is very weak, with its maximum being only $0.03\,\mathrm{m\,s^{-1}}$, but the downdraft occupying a narrower region on the downwind side is relatively strong, with its maximum being $-0.13\,\mathrm{m\,s^{-1}}$ (Fig. 5). There also exists relatively strong updraft in the region close to the downwind building edge (Fig. 5), which results from flow impingement on the downwind building edge. A trajectory analysis for an even-notch configuration in a wind tunnel by Hoydysh and Dabberdt (1988) shows that a bubble exits the canyon near the downwind model-building edge (Fig. 10 in their paper), indicating an updraft there. This is consistent with our numerical result. The turbulent kinetic energy changes very little across the top of the canyon, except for the region near the downwind building edge where it increases toward the building edge (Fig. 5).

Next, the spatial distributions of pollutant concentration and its budget, especially across the top of the street canyon, are investigated. At $t = 2$ h, the pollutant concentration at each grid point reaches a quasi-steady state. The pollutant concentration field at $t = 2$ h (Fig. 6) exhibits higher concentration on the upwind side than on the downwind side, as shown in many previous studies (e.g., Hoydysh and Dabberdt, 1988; Baik and Kim, 1999). This feature is directly linked to the vortex circulation within the canyon, which causes pollutants emitted from the street-level source to be transported upwind and then upward. Pollutants are escaping from the street canyon by mechanisms that will be described later. At $t = 2$ h, the calculated residue concentration ratio, a ratio of the pollutant amount remaining within the canyon to the total emitted pollutant amount, is 0.08.

Fig. 7 shows the horizontal distributions of pollutant concentration (C), its horizontal and vertical gradients ($\partial C/\partial x$ and $\partial C/\partial z$), and turbulent eddy diffusivity for pollutants (K_c) at $z = 40$ m. In this study, K_c is calculated using

$$K_c = \frac{K_m}{Sc_t} = \frac{C_\mu k^2}{Sc_t\,\varepsilon}, \tag{4}$$

where K_m is the turbulent eddy diffusivity for momentum, k is the turbulent kinetic energy, and ε is the dissipation rate. Sc_t is the turbulent Schmidt number and specified as 0.9 (Sini et al., 1996). At the roof level, the pollutant concentration is higher near the canyon center than near the upwind or downwind side. The concentration near the downwind building is high compared with that near the upwind building. The horizontal gradient of the concentration is positive on the upwind side and decreases to zero as going to the downwind building. Near the canyon center and on the downwind side, the horizontal gradient is very small, except for the region close to the downwind building where its magnitude is large with negative gradient. As expected, the vertical gradient of the concentration is negative everywhere. Its magnitude increases rapidly from the upwind building edge to $x = 34$ m and then decreases gradually. The turbulent eddy diffusivity for pollutants increases toward the downwind building mainly due to the increase of the turbulent kinetic energy toward the downward building. The average value of K_c cross the canyon top is $0.39\,\mathrm{m^2\,s^{-1}}$.

The transport equation for C can be written as

$$\frac{\partial C}{\partial t} = -U\frac{\partial C}{\partial x} - W\frac{\partial C}{\partial z} + \frac{\partial}{\partial x}\left(K_c\frac{\partial C}{\partial x}\right) + \frac{\partial}{\partial z}\left(K_c\frac{\partial C}{\partial z}\right) + S_c, \tag{5}$$

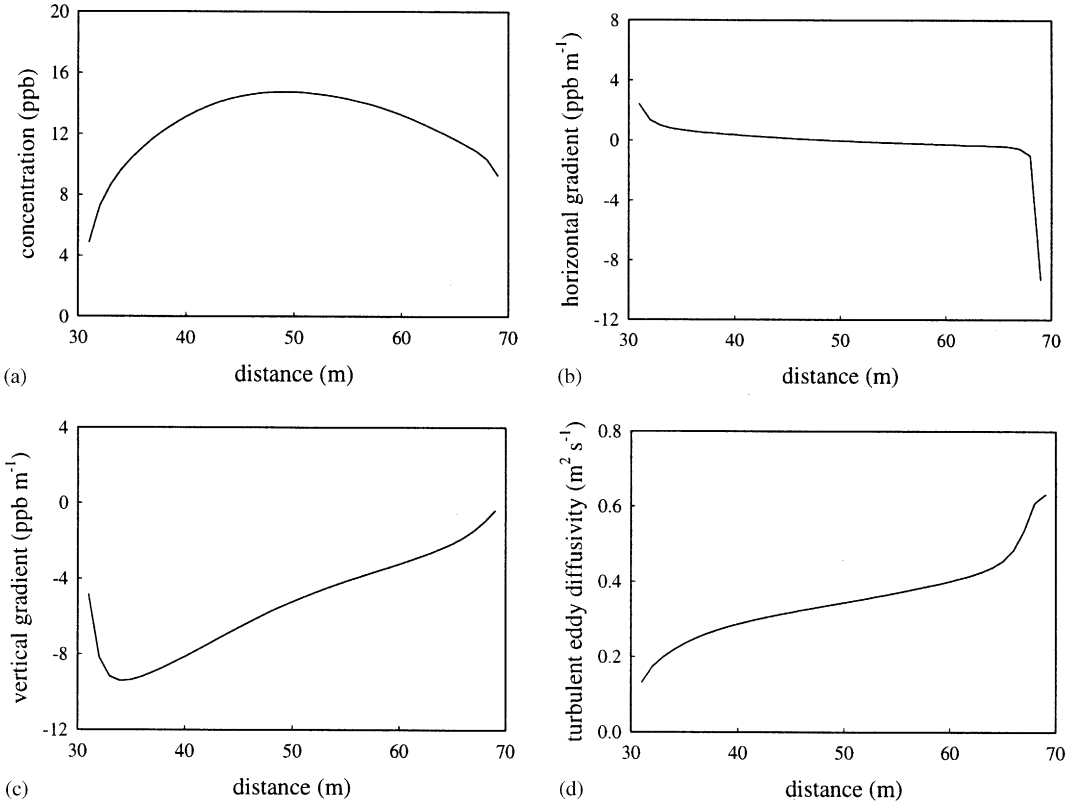

Fig. 7. Horizontal distributions of (a) pollutant concentration, (b) horizontal gradient of pollutant concentration, (c) vertical gradient of pollutant concentration, and (d) turbulent eddy diffusivity for pollutants at $z = 40$ m. These are at $t = 2$ h.

where U and W are the mean horizontal and vertical velocities, respectively, and S_c is the source or sink term of pollutants. The horizontal distributions of horizontal and vertical advection and diffusion terms at the canyon top are plotted in Fig. 8. On the upwind side, the horizontal advection of C is negative ($U > 0$ and $\partial C/\partial x > 0$) and the vertical advection term is positive ($W > 0$ and $\partial C/\partial z < 0$). Thus, the horizontal advection acts to reduce the concentration, while the vertical advection acts to increase the concentration. On the downwind side, on the other hand, the positive horizontal advection ($U > 0$ and $\partial C/\partial x < 0$) and the negative vertical advection ($W < 0$ and $\partial C/\partial x < 0$) act to increase and reduce the concentration, respectively. Near the canyon center, the contribution of horizontal advection to the tendency of C is small compared with other regions because $\partial C/\partial x$ is very small (Fig. 7b), although the horizontal wind speed is large there (Fig. 5). The horizontal diffusion term is virtually negligible across the canyon top, except for the regions close to the building edges where diffused pollutants in the horizontal direction act to reduce the concentration ($\partial C/\partial t < 0$). The vertical diffusion term is positive on the upwind side. On the downwind side, the vertical diffusion term is negative and its magnitude is small compared with that on the upwind side.

Now, the process responsible for pollutant escape from the urban street canyon is investigated. For this purpose, the vertical flux of pollutants by mean flow (F_m) and the vertical flux of pollutants by turbulent flow (F_t) are calculated using

$$F_m = CW, \tag{6}$$

$$F_t = \overline{cw} = -K_c \frac{\partial C}{\partial z}, \tag{7}$$

where c is the deviation from the mean concentration and w is the deviation from the mean vertical velocity. Fig. 9 shows the horizontal distributions of F_m and F_t at $z = 40$ m. The horizontal pattern of the vertical mean flux (F_m) is very similar to that of the vertical velocity (Fig. 5). The vertical mean flux is positive (that is, pollutants escape from the street canyon) from the upwind building edge to $x = 52$ m, negative (pollutants go into the canyon) up to $x = 68$ m, and again positive up to the downwind building edge. The maximum

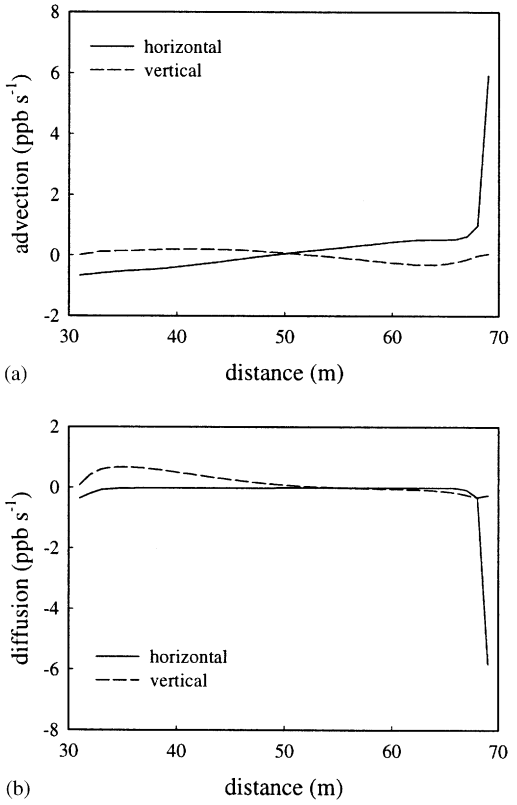

Fig. 8. Horizontal distributions of (a) horizontal (solid line) and vertical (dashed line) advection terms and (b) horizontal (solid line) and vertical (dashed line) diffusion terms at $z = 40$ m in the transport equation for pollutant concentration. These are at $t = 2$ h.

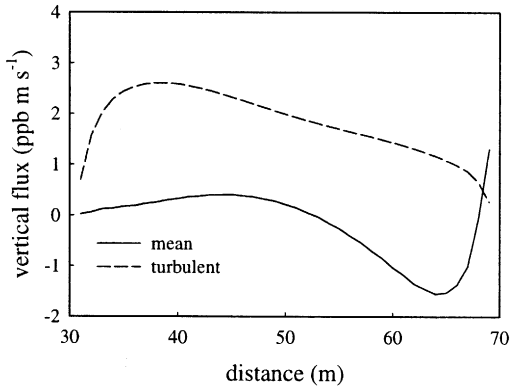

Fig. 9. Horizontal distributions of vertical mean flux of pollutants and vertical turbulent flux of pollutants at $z = 40$ m. These are at $t = 2$ h.

upward and downward mean fluxes are 0.40 ppb m s^{-1} at $x = 45$ m and -1.55 ppb m s^{-1} at $x = 64$ m, respectively. These locations approximately correspond to the maximum updraft and downdraft locations at the roof level. The vertical turbulent flux (F_t) is upward everywhere. The upward vertical turbulent flux increases from the upwind building edge to $x = 38$ m and then gradually decreases toward the downwind building edge. The maximum upward turbulent flux is 2.61 ppb m s^{-1} at $x = 38$ m, where the product of the turbulent eddy diffusivity for pollutants and the vertical concentration gradient is largest in its magnitude (Fig. 7).

Fig. 9 indicates that the magnitude of the vertical turbulent flux is much larger than that of the vertical mean flux and that pollutants escape from the street canyon mainly by turbulent transfer process, not by transfer process by mean flow. To examine net pollutant fluxes across the canyon top, the vertical mean and turbulent fluxes are integrated horizontally from $x = 30$ to 70 m at $z = 40$ m. That is, the horizontally integrated vertical mean and turbulent fluxes are, respectively, given by

$$\beta_m = \int_L F_m \, dx, \tag{8}$$

$$\beta_t = \int_L F_t \, dx. \tag{9}$$

The calculated net fluxes are $\beta_m = -6.57$ ppb m^2 s^{-1} and $\beta_t = 70.63$ ppb m^2 s^{-1}. Hence, the net effect of turbulent process is to transport pollutants from the canyon into the above-canyon region but the net effect by mean flow is to cause some escaped pollutants to reenter the canyon. Each contribution of updraft and downdraft to β_m is calculated. This gives $\beta_m^+ = 6.82$ ppb m^2 s^{-1} in the updraft region and $\beta_m^- = -13.40$ ppb m^2 s^{-1} in the downdraft region. This means that the amount of pollutants escaping from the canyon by updraft is smaller than that coming into the canyon by downdraft.

The results presented above (control experiment) show that at the roof level of the street canyon, pollutants escape mainly by turbulent process and the net vertical flux of pollutants by mean flow is even downward. To further investigate the validity of these findings, some experiments are undertaken. Table 1 describes the experimental condition that deviates from the control experiment and lists average turbulent eddy diffusivity for pollutants and the horizontally integrated vertical mean and turbulent fluxes of pollutants at the top of the street canyon. Note that in the control experiment, $a = 0.005$ [see Eq. (2)], $U_r = 2.5$ m s^{-1} [see Eq. (1)], and $\delta = 1$ (street aspect ratio).

The first two experiments in Table 1 are on the inflow turbulence intensity. Here, a is set equal to one-fifth (0.001, S1 experiment) and five times (0.025, S2 experiment) the value in the control experiment. As a increases (that is, the inflow turbulence intensity increases), the average turbulent eddy diffusivity for pollutants at the roof level of the street canyon ($\bar{K}_c$) increases because of increasing turbulent kinetic energy

Table 1
Average turbulent eddy diffusivity for pollutants ($\bar{K}_c$) and horizontally integrated vertical mean (β_m) and turbulent (β_t) fluxes at the top of street canyon in each of numerical experiments S1–S6[a]

	Experimental description	$\bar{K}_c$ ($m^2 s^{-1}$)	β_m (ppb $m^2 s^{-1}$)	β_t
Control	Control experiment	0.39	−6.57	70.63
S1	Lower inflow turbulence intensity ($a = 0.001$)	0.32	−7.22	69.72
S2	Higher inflow turbulence intensity ($a = 0.025$)	0.56	−5.47	71.27
S3	Weaker inflow wind speed ($U_r = 1.25\,m\,s^{-1}$)	0.19	−5.25	64.14
S4	Stronger inflow wind speed ($U_r = 5\,m\,s^{-1}$)	0.78	−6.89	73.69
S5	Larger street aspect ratio ($\delta = 2$)	0.48	−0.33	3.56
S6	Isolated buildings	2.97	14.58	60.25

[a]The parameter values in these simulations are the same as those in the control experiment, except for the value indicated in the experimental description. In the control experiment, $a = 0.005$, $U_r = 2.5\,m\,s^{-1}$, and $\delta = 1$. Note that the adjectives lower, higher, weaker, etc., in this table are used relative to the values used in the control experiment.

[see Eq. (4)]. The horizontally integrated vertical mean flux at the roof level of the street canyon (β_m) is negative in the S1 and S2 experiments, meaning that the net vertical pollutant transport by mean flow is downward at the roof level. The magnitude of β_m decreases with increasing inflow turbulence intensity. The horizontally integrated vertical turbulent flux at the roof level of the street canyon (β_t) is positive in the S1 and S2 experiments, that is, turbulent process makes pollutants escape from the canyon. As the inflow turbulence intensity increases, β_t increases. In spite of a large increase in $\bar{K}_c$ with increasing inflow turbulence intensity, the increase in β_t is very small. This is because the magnitude of the vertical gradient of pollutant concentration becomes small with increasing inflow turbulence intensity by the turbulent mixing of pollutants and also because the pollutant concentration becomes low with increasing inflow turbulence intensity. The magnitude of β_t in the S1 or S2 experiment is much larger than that of β_m.

The next two experiments are concerned with the inflow wind speed, in which U_r is set equal to $1.25\,m\,s^{-1}$ in the S3 experiment (half the value in the control experiment) and to $5\,m\,s^{-1}$ in the S4 experiment (twice the value in the control experiment). As the inflow wind speed increases, the vortex in the street canyon becomes intense and accordingly the magnitude of β_m increases. $\bar{K}_c$ and β_t also increases with increasing inflow wind speed. As in the S1 and S2 experiments, the magnitude of β_t in the S3 or S4 experiment is much larger than that of β_m.

According to Eq. (2), the inflow turbulent kinetic energy is proportional to the square of the inflow wind speed. Therefore, the S3 and S4 experiments are actually different from the control experiment in that the inflow turbulence intensity as well as the inflow wind speed varies. The difference in $\bar{K}_c$ between the S4 experiment (twice inflow wind speed and four times inflow turbulence intensity) and the control experiment ($0.39\,m^2 s^{-1}$) is 2.3 times larger than that between the S2 experiment (five times inflow turbulence intensity) and the control experiment ($0.17\,m^2 s^{-1}$). This implies that the increase of the inflow wind speed only in the S4 experiment contributes to the increase of $\bar{K}_c$. A similar argument can be made for β_t. The result that the magnitude of β_m decreases when the inflow turbulence intensity increases ($\beta_m = -6.57$ ppb $m^2 s^{-1}$ in the control experiment and -5.47 ppb $m^2 s^{-1}$ in the S2 experiment) suggest that the increase of the inflow turbulence intensity due to the increase of the inflow wind speed in the S4 experiment should contribute to the decrease of the magnitude of β_m. However, the magnitude of β_m in the S4 experiment is larger than that of the control experiment. These imply that the increase of the inflow wind speed only in the S4 experiment contributes the increase of the magnitude of β_m. Parallel arguments can be made using the results from the control, S1, and S3 experiments in Table 1. Therefore, the main findings from the S3 and S4 experiments mentioned in the previous paragraph are still valid.

In the S5 experiment, the building height is 80 m and the width between the two buildings is the same as that in the control experiment (40 m). Hence, the street aspect ratio in the S5 experiment is 2.When the street aspect ratio is 2, two counter-rotating vortices are formed in the street canyon and the intensity of the upper vortex is stronger than that of the lower vortex. In the lower region of the street canyon, the concentration is higher near the downwind building than near the upwind building because of the pollutant transport by the counterclockwise-rotating lower vortex. On the other hand, in the upper region of the canyon, the concentration is higher near the upwind building than near the downwind building because of the pollutant transport by the clockwise-rotating upper vortex. $\bar{K}_c$ in the S5 experiment is larger than that in the control experiment with a street aspect ratio of 1. The sign of β_m is negative.

The pollutant concentration at the roof level in the S5 experiment ($z = 80$ m) is much lower than that in the control experiment ($z = 40$ m). Therefore, the magnitude of β_m (or β_t) in the S5 experiment is much smaller than that in the control experiment. So, the natural ventilation becomes poor in a street canyon with larger street aspect ratio. The sign of β_t is positive and its magnitude is much larger than that of β_m. The results from the S1–S5 experiments essentially confirm the main findings from the control experiment.

The flow above the street canyon in the control and S1–S5 experiments is parallel to the ground because the inflow above the upwind building is parallel to the ground. However, when there are two isolated buildings, flow separation can occur at the upwind edge of the upwind building. Hence, the flow above the street canyon cannot be parallel to the ground but can have a streamline curvature. To examine the impact on pollutant escape in this case, an experiment with two isolated buildings with a separation distance of 40 m is performed. In this experiment (S6 experiment), the building width is 30 m (so the building aspect ratio is 4/3 and the street aspect ratio is 1) and the horizontal domain size is 300 m, with the horizontal center of the street canyon being that of the model domain. Other experimental conditions are the same as those in the control experiment. In the S6 experiment, because of the flow separation, the vortex is not completely trapped within the canyon but the vortex center is shifted a little upward and some part of the vortex appears slightly above the canyon. The mean updraft at the roof level becomes strong compared with that of the control experiment. This results in a positive value of β_m, that is, a net upward vertical flux by mean flow at the roof level. The magnitude of β_m is larger than that of the control experiment, while the magnitude of β_t is smaller. Considering β_m and β_t together, the natural ventilation in the street canyon improves in the case of the isolated building configuration compared with the case of the building configuration in the control experiment.

5. Summary and conclusion

This study examined pollutant transport from urban street canyons using a two-dimensional flow and dispersion model. It was shown that pollutants escape from the street canyon mainly by turbulent process and that the net contribution of mean flow is to make some escaped pollutants reenter the street canyon. These results were further confirmed by the experiments with different inflow turbulence intensities, inflow wind speeds, and street aspect ratio. In the experiment with two isolated buildings, the horizontally integrated vertical flux of pollutants by mean flow at the roof level of the street canyon was upward due to flow separation but the other main results were the same as those from the other experiments.

In this study, the ambient flow was considered to be perpendicular to the street. In reality, the direction of the ambient flow to the street varies and can have a significant influence on flow and dispersion, depending on its direction. A three-dimensional numerical study is needed to examine whether the present results obtained in two dimensions on the escape of pollutants from urban street canyons remain valid in three dimensions.

Acknowledgements

The authors are very grateful to two anonymous reviewers for providing valuable comments on this study. Part of this research was performed while the first author was visiting the Department of Applied Mathematics and Theoretical Physics, University of Cambridge, UK, on his sabbatical leave. He would like to thank Dr. Francois Caton for providing valuable comments on urban flow and dispersion research. This research was supported by the Climate Environment System Research Center sponsored by the SRC Program of the Korea Science and Engineering Foundation. This research was also supported by the Brain Korea 21 Program.

References

Baik, J.-J., Kim, J.-J., 1999. A numerical study of flow and pollutant dispersion characteristics in urban street canyons. Journal of Applied Meteorology 38, 1576–1589.

Baik, J.-J., Park, R.-S., Chun, H.-Y., Kim, J.-J., 2000. A laboratory model of urban street-canyon flows. Journal of Applied Meteorology 39, 1592–1600.

DePaul, F.T., Sheih, C.M., 1985. A tracer study of dispersion in an urban street canyon. Atmospheric Environment 19, 555–559.

Hotchkiss, R.S., Harlow, F.H., 1973. Air pollution transport in street canyons. EPA-R4-73-029.

Hoydysh, W.G., Dabberdt, W.F., 1988. Kinematics and dispersion characteristics of flows in asymmetric street canyons. Atmospheric Environment 22, 2677–2689.

Hunter, L.J., Johnson, G.T., Watson, I.D., 1992. An investigation of three-dimensional characteristics of flow regimes within the urban canyon. Atmospheric Environment 26B, 425–432.

Kastner-Klein, P., Fedorovich, E., Sini, J.-F., Mestayer, P.G., 2000. Experimental and numerical verification of similarity concept for dispersion of car exhaust gases in urban street canyons. Environmental Monitoring and Assessment 65, 353–361.

Kim, J.-J., Baik, J.-J., 1999. A numerical study of thermal effects on flow and pollutant dispersion in urban street canyons. Journal of Applied Meteorology 38, 1249–1261.

Lee, I.Y., Park, H.M., 1994. Parameterization of the pollutant transport and dispersion in urban street canyons. Atmospheric Environment 28, 2343–2349.

Meroney, R.N., Pavageau, M., Rafailidis, S., Schatzmann, M., 1996. Study of line source characteristics for 2-D physical modelling of pollutant dispersion in street canyons. Journal of Wind Engineering and Industrial Aerodynamics 62, 37–56.

Nicholson, S.E., 1975. A pollution model for street-level air. Atmospheric Environment 9, 19–31.

Odell, G.M., Kovasznay, L.S.G., 1971. A new type of water channel with density stratification. Journal of Fluid Mechanics 50, 535–543.

Patankar, S.V., 1980. Numerical Heat Transfer and Fluid Flow. McGraw-Hill, New York, 197pp.

Sini, J.-F., Anquetin, S., Mestayer, P.G., 1996. Pollutant dispersion and thermal effects in urban street canyons. Atmospheric Environment 30, 2659–2677.

Uehara, K., Murakami, S., Oikawa, S., Wakamatsu, S., 2000. Wind tunnel experiments on how thermal stratification affects flow in and above urban street canyons. Atmospheric Environment 34, 1553–1562.

Wedding, J.B., Lombardi, D.J., Cermak, J.E., 1977. A wind tunnel study of gaseous pollutants in city street canyons. Journal of the Air Pollution Control Association 27, 557–566.